

UCLA

UCLA Previously Published Works

Title

Continuous wave operation of buried heterostructure 4.6 μm quantum cascade laser Y-junctions and tree arrays.

Permalink

<https://escholarship.org/uc/item/28t8q98h>

Journal

Optics Express, 22(1)

ISSN

1094-4087

Authors

Lyakh, Arkadiy
Maulini, Richard
Tsekoun, Alexei
[et al.](#)

Publication Date

2014-01-13

DOI

10.1364/oe.22.001203

Copyright Information

This work is made available under the terms of a Creative Commons Attribution-NonCommercial License, available at <https://creativecommons.org/licenses/by-nc/4.0/>

Peer reviewed

Continuous wave operation of buried heterostructure 4.6 μ m quantum cascade laser Y-junctions and tree arrays

Arkadiy Lyakh,¹ Richard Maulini,¹ Alexei Tsekoun,¹ Rowel Go,¹
and C. Kumar N. Patel^{1,2,*}

¹Pranalytica, Inc., 1101 Colorado Ave., Santa Monica, California 90401, USA

²Department of Physics & Astronomy, University of California, Los Angeles, California 90095, USA

*patel@pranalytica.com

Abstract: Room-temperature continuous-wave operation for buried heterostructure 4.6 μ m quantum cascade laser Y-junctions and tree arrays, overgrown using hydride vapor phase epitaxy, has been demonstrated. Pulsed wall plug efficiency for the Y-junctions with bending radius of 5mm was measured to be very similar to that of single-emitter lasers from the same material, indicating low coupling losses. Comparison between model and experimental data showed that the in-phase mode was dominating for 10mm-long Y-junctions with 5 μ m-wide 1mm-long stem and 5 μ m-wide branches. Total optical power over 1.5W was demonstrated for four-branch QCL tree array.

©2014 Optical Society of America

OCIS codes: (140.5965) Semiconductor lasers, quantum cascade; (140.3298) Laser beam combining.

References and links

1. A. Lyakh, R. Maulini, A. Tsekoun, R. Go, C. Pflügl, L. Diehl, Q. Wang, F. Capasso, and C. K. N. Patel, "3 W continuous-wave room temperature single-facet emission from quantum cascade lasers based on nonresonant extraction design approach," *Appl. Phys. Lett.* **95**(14), 141113 (2009).
2. Y. Bai, N. Bandyopadhyay, S. Tsao, S. Slivken, and M. Razeghi, "Room temperature quantum cascade lasers with 27% wall plug efficiency," *Appl. Phys. Lett.* **98**(18), 181102 (2011).
3. R. Maulini, A. Lyakh, A. Tsekoun, and C. K. N. Patel, " λ -7.1 μ m quantum cascade lasers with 19% wall-plug efficiency at room temperature," *Opt. Express* **19**(18), 17203–17211 (2011).
4. A. Lyakh, R. Maulini, A. Tsekoun, R. Go, and C. K. N. Patel, "Multiwatt long wavelength quantum cascade lasers based on high strain composition with 70% injection efficiency," *Opt. Express* **20**(22), 24272–24279 (2012).
5. A. Lyakh, R. Maulini, A. Tsekoun, R. Go, and C. K. N. Patel, "Tapered 4.7 μ m quantum cascade lasers with highly strained active region composition delivering over 4.5 watts of continuous wave optical power," *Opt. Exp.* **20**(4), 4382 (2012).
6. A. Lyakh, R. Maulini, A. Tsekoun, R. Go, S. Von Der Porten, C. Pflugl, L. Diehl, F. Capasso, and C. K. N. Patel, "High-performance continuous-wave room temperature 4.0- μ m quantum cascade lasers with single-facet optical emission exceeding 2 W," *Proc. Natl. Acad. Sci. U. S. A.* **107**(44), 18799–18802 (2010).
7. L. K. Hoffmann, M. Klinkmüller, E. Mujagić, M. P. Semtsiv, W. Schrenk, W. T. Masselink, and G. Strasser, "Tree array quantum cascade laser," *Opt. Express* **17**(2), 649–657 (2009).
8. S. Lourduos and O. Kjebon, "Hydride vapour phase epitaxy revisited," *IEEE Sel. Top. Quantum Electron.* **3**(3), 749–767 (1997).
9. L. K. Hoffmann, C. A. Hurni, S. Schartner, M. Austerer, E. Mujagić, M. Nobile, A. Benz, W. Schrenk, A. M. Andrews, P. Klang, and G. Strasser, "Coherence in Y-coupled quantum cascade lasers," *Appl. Phys. Lett.* **91**(16), 161106 (2007).

1. Introduction

Quantum cascade laser (QCL) performance has been radically improving over the last five years, with multi-watt continuous wave (CW) room temperature operation now demonstrated in both mid-wave and long-wave infrared spectral regions [1–6]. Further improvement in wallplug efficiency and more advanced cavity designs, such as tapered waveguide geometry, promises to increase the single-ended optical power output from single emitters in the near future. Nonetheless, coherent or spectral beam combining of multiple emitters will be

necessary to reach power levels in excess of about 5 W, the maximum CW/RT power presently believed to be achievable from a single emitter, while maintaining a good beam quality.

Being insensitive to shock/vibration and structural distortions, monolithic beam combining configurations are very attractive for demanding field applications. In ideal case, a monolithic configuration should be fully compatible with the optimized active region/waveguide design of state-of-the-art single emitters, i.e. unaltered active region, all-InP waveguide, and iron-doped InP overgrowth necessary for the buried heterostructure (BH) geometry. Monolithic arrays have been extensively studied for diode lasers. However, not all of these configurations are applicable to QCLs without significant changes in the optimized QCL design. In particular, semi-insulating InP overgrowth for QCLs, required for efficient lateral active region heat extraction, creates a strong lateral waveguide with $\Delta n > 0.05$ (for diode lasers $\Delta n \approx 10^{-3}$). As a consequence, array configurations based on evanescent coupling or anti-guiding cannot be used for QCLs with all-InP overgrowth.

An alternative monolithic configuration is a so-called ‘tree configuration’ based on Y-junctions (Fig. 1). In this configuration, several emitters (branches) are brought together by an array of Y-junctions into a single waveguide, the stem. All the elements, as well as Y-junctions and the stem, are single-mode waveguides that are uniformly pumped. Through the Y-junctions the elements merge together at the back facet. This ensures parallel coupling between the elements that entails in-phase mode dominance and, as a consequence, leads to an on-axis far-field intensity distribution with nearly diffraction-limited divergence.

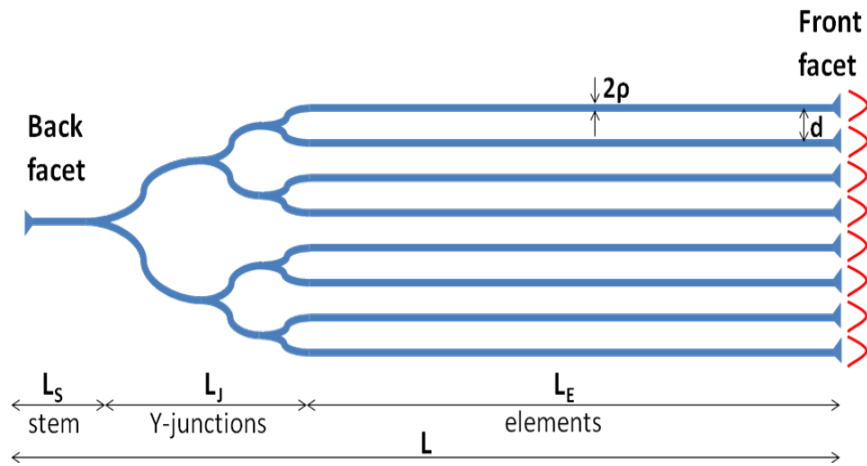


Fig. 1. Schematic of the tree-array configuration. L_S , L_J , and L_E are length of stem, Y-junction coupling section, and elements (branches), respectively, $2p$ is width of the elements, and d is interelement spacing.

Pulsed operation of long-wave infrared ridge waveguide (RWG) QCL tree arrays with branches of different length was demonstrated for QCLs emitting at $10\mu\text{m}$ [7]. While far-field measurements showed that in-phase fundamental mode was dominant for these devices, measured slope efficiency was low. As a consequence, brightness for these RWG QCL tree arrays did not exceed that for single emitters. This was in part attributed to modal competition among branches of different length.

Realization of efficient mid-wave infrared (MWIR) RWG QCL tree arrays with dominating in-phase mode may be problematic: because of the strong lateral waveguide, characteristic to the RWG configuration, ridge width for the cut-off condition of the first order mode in the stem is less than $3\mu\text{m}$ that is difficult to achieve. As a consequence, the out-of-phase mode can be suppressed only through increased waveguide losses discrimination between the first and zero order modes of the stem. This, however, also leads to increased

losses for the in-phase mode and, therefore, reduces overall laser performance. In-phase mode operation for BH tree arrays, on the other hand, should be achievable through discrimination in mode overlap factor with the active region, with relatively unaffected overlap factor for the zero order mode under the cut-off conditions for the first order mode. Therefore, BH configuration is preferential for MWIR QCL tree arrays. This configuration also offers the advantages of lower sidewall scattering, especially for shorter wavelengths QCLs, and lower thermal resistance that is important for CW operation. In this work we demonstrate CW room temperature operation of first MWIR BH QCL tree arrays with branches of the same length.

2. Wafer processing

The critical challenge in realization of BH QCL tree-arrays is buried heterostructure overgrowth in the coupling area. The metal organic chemical vapor deposition (MOCVD) overgrowth technique that is routinely used for QCLs is a selective growth process. The ultimate surface morphology for MOCVD overgrowth depends on many factors, including mask undercut, growth conditions and selective-growth enhancements. It may be difficult to control the mask undercut in the vicinity of the merging branches of the Y-junctions. Also, in this region the two masks merge, so that locally the masked area is greater. This may cause an enhancement to the growth rate in the vicinity of the merge, which compromises overgrowth planarity. Therefore, MOCVD may not be the best overgrowth technique for the tree-array configuration.

Instead of MOCVD, we chose Hydride Vapor Phase Epitaxy (HVPE) [8], an alternative overgrowth technique. One of HVPE's main strengths is its ability to produce complete planarization, regardless of the mesa orientation and height. For the first demonstration of CW BH MWIR QCL tree arrays we used a 4.6 μm quantum cascade laser material with active region/waveguide design similar to that in [1]. After MBE-growth of epi-layers the wafer was processed into semi-insulating BH configuration using HVPE. SEM pictures for the BH material are shown in Figs. 2(a) and 2(b). Figure 2(a) is a cross sectional SEM picture of a four element tree array that demonstrates excellent overgrowth quality without any visible voids or formation of so-called 'rabbit ears', overgrowth defects that protrude above the surface of the wafer along mesa edges. Figure 2(b) shows that even in the merge section, where mask undercut was difficult to control, overgrowth quality was still very good. The overall non-planarity of the wafer surface is the result of non-ideal overgrowth thickness calibration, and can be easily corrected in future runs.

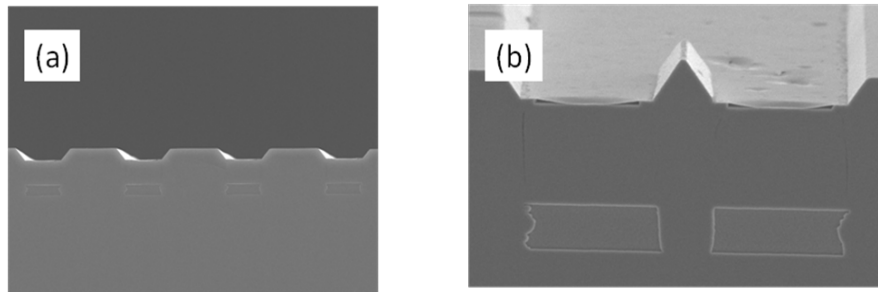


Fig. 2. (a) Cross sectional SEM picture of a four element array. Active region thickness – 1.8 μm ; interelement spacing - 10 μm (b) cross sectional SEM picture of a Y-junction at the merge section. Active region thickness – 1.8 μm ; interelement spacing - 2 μm .

3. Experimental data for Y-junction QCLs

Y-junctions are the building blocks of tree arrays and they need to be analyzed first. Figure 3 compares the room temperature pulsed optical power vs. current characteristics of a 10mm single-element BH QCL, and a $L = L_S + L_J + L_E = 10\text{mm}$ BH Y-junction QCL, processed at the same time. Y-junction geometrical parameters were: stripe width both for branches and the stem equal to $2\rho = 5\mu\text{m}$ (flared to 10 μm at the facets with taper angle of 1 $^\circ$), stem length

equal to $L_S = 1\text{ mm}$, bending radius of 5 mm , and inter-element spacing equal to $d = 10\ \mu\text{m}$. As evident from the figure, WPE of the Y-junction QCL is approximately the same as for the single-element device and combined optical power from the stem and branches ends of the Y-junction was increased proportionally to the pumped area. This is a very important result demonstrating that coupling losses are small and the relatively short coupling sections with small bending radii can be used for MWIR BH QCL tree arrays.

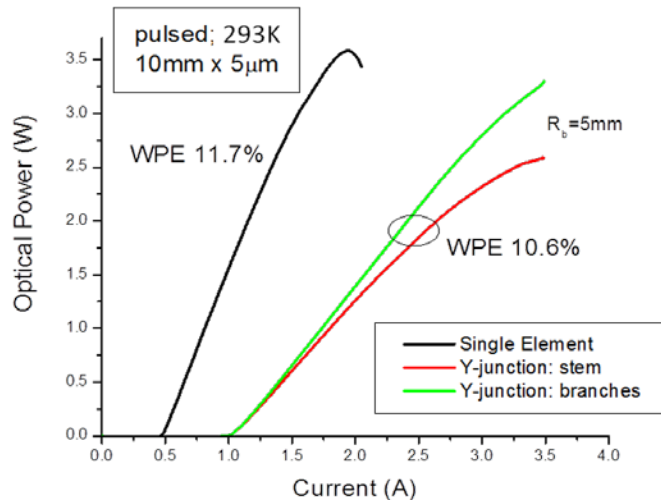


Fig. 3. Pulsed optical power vs. current characteristics of a $5\ \mu\text{m} \times 10\text{ mm}$ single-element and 10 mm Y-junction with bending radius R_b of 5 mm and $5\ \mu\text{m}$ -thick branches and stem.

Figure 4(a) shows near field (NF) intensity distribution of a Y-junction QCL in CW operation at 1.9 A . Slight asymmetry in intensity distribution between the two branches was most probably processing related and can be corrected in future. Figure 4(b) shows measured (triangles) and calculated (solid red line) far field (FF) intensity distributions for the same laser under the same conditions. The excellent agreement between model and experiment shows that the beam is diffraction limited and it is a result of two in-phase waves emitted by the two Y-junction branches. Side-lobes in the FF can be further suppressed by increasing NF fill-factor, i.e. ratio of NF beam size to the distance between the branches.

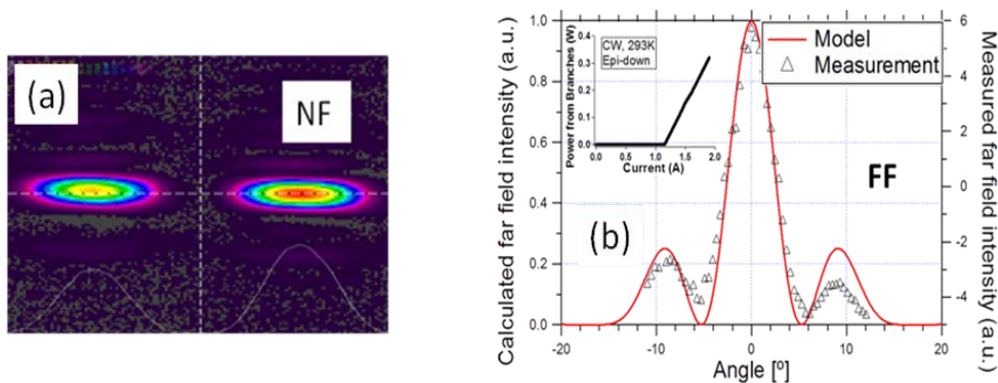


Fig. 4. (a) Near field intensity distribution at the laser facet of a Y-junction QCL (CW operation). (b) CW Far field intensity distribution for the same laser as in Fig. 4(a) taken at 1.9 A . Triangles – experiment, solid red line – model. Inset shows CW optical power vs. current characteristics.

4. Experimental data for 4-element QCL tree arrays

Figure 5 shows light and voltage vs. current (LIV) characteristics in CW operation of a four-element tree array QCL with bending radius of 20mm and otherwise the same parameters as for the Y-junction. Optical power of over 1.5W was demonstrated for this device. The laser driving current, and, therefore, optical power were limited by the current driver. The power vs current characteristic exhibited irregularities that are usually associated with mode-hopping. Far-field measurements confirmed this observation. Comparison between experimental and theoretical far-field data, presented in Fig. 6, demonstrates that, in contrast to Y-junctions where in-phase mode was dominating, four-element array with the current design supported a mixture of in-phase and out-of-phase modes, which distorted the far field. We also observed that the far field was constantly changing with current. This result indicated that the stem section in the present configuration of the four-element array did not effectively suppress the out-of-phase mode. As discussed in [9], coupling efficiency for Y-junctions is higher for the out-of-phase mode. Therefore, a larger number of merging sections required to couple larger number of elements favors out-of-phase mode operation. To compensate for this effect, stem section dimensions need to be adjusted to suppress the out-of-phase mode. This can be achieved by either making the stem section longer or by making it narrower. This will be implemented in our future work.

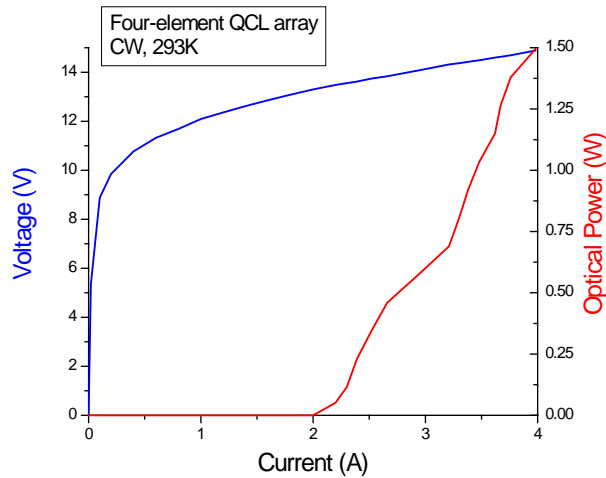


Fig. 5. L-I-V characteristics of a four-element QCL tree array. Optical power was limited by the current driver.

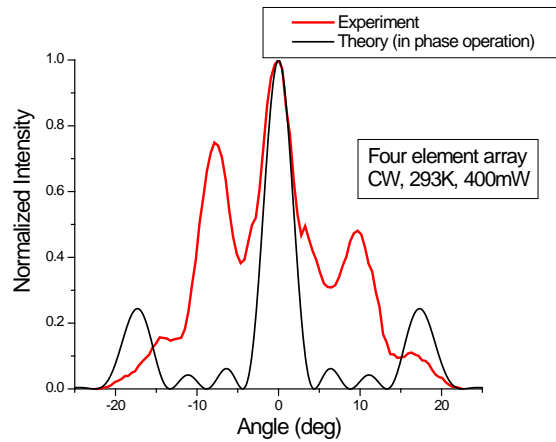


Fig. 6. Far field intensity distribution for the same laser as in Fig. 5 (CW operation; 400mW). Red line – experiment, black line – model.

6. Conclusion

In conclusion, we demonstrated first CW operation of MWIR BH QCL Y-junctions and tree arrays. Low coupling losses and in-phase mode operation with diffraction limited divergence were demonstrated for Y-junctions with the design described above. Four-branch QCL arrays, utilizing the Y-junction design, delivered over 1.5W in continuous wave mode at room temperature. Out-of-phase mode has to be further suppressed for BH QCL tree arrays with a large number of merges to achieve on-axis, diffraction-limited beam.